Available online at www.sciencedirect.com
SCIENCE DIRECT®
Catalysis Today 96 (2004) 179–186
CATALYSIS TODAY
www.elsevier.com/locate/cattod

Vanadium oxide supported on mesoporous Al_2O_3 Preparation, characterization and reactivity

P. Concepción, M.T. Navarro, T. Blasco, J.M. López Nieto*, B. Panzacchi[1], F. Rey

Instituto de Tecnología Química, UPV-CSIC, Avenida de los Naranjos s/n, 46022 Valencia, Spain

Available online 24 August 2004

Abstract

The application of different techniques (diffuse reflectance-UV–vis, ^{51}V NMR, FT-IR of adsorbed pyridine and TPR-H_2) in the characterization of vanadia supported on mesoporous Al_2O_3 catalysts shows that the nature of the vanadium species depends on the V-loading. At V-content lower than 15 wt.% of V-atoms (30% of the theoretical monolayer), vanadium is mainly in a tetrahedral environment. Higher V-contents in the catalyst leads to the formation of octahedral V^{5+} species and V_2O_5-like species. Both XRD and textural results indicate that the mesoporous structure of the support is mostly maintained after the vanadium incorporation, and therefore high surface areas were obtained on the final catalysts. Al_2O_3-suppported vanadia catalysts are active and selective in the oxidative dehydrogenation of ethane, although the catalytic behavior depends on the V-loading. High rates of formation of ethylene per unit mass of catalyst per unit time have also been observed as a consequence of the high dispersion of V-atoms on the surface of the support.

Keywords: Ethane oxidative dehydrogenation to ethylene; Vanadium oxide supported on mesoporous alumina; Catalyst characterization; X-ray diffraction; Infrared spectroscopy of adsorbed–desorbed pyridine; TPR; Diffuse reflectance-UV–vis; ^{51}V NMR

1. Introduction

Supported vanadium oxide exhibits interesting catalytic performance depending on the kind of support, the vanadium content, and the preparation method [1–7]. This is the case of the oxidative dehydrogenation (ODH) of short chain alkanes in which the selectivity to olefins depends on the metal oxide support and the alkane feed [1–3]. So, vanadium oxide incorporated on metal oxide supports with basic character is selective in the ODH of *n*-butane to butenes and butadiene, while supports with acid character are preferred in the ODH of ethane [1,8–10]. The behavior of these catalysts in the ODH of propane is intermediate between those observed in the ODH of ethane and butane [1,8–10].

Al_2O_3-supported vanadia catalysts have been reported to be one of the most active catalysts in the ODH of short chain alkanes [6], especially in ODH of ethane [10–12] and propane [13–15]. Their catalytic behavior can be improved by the incorporation of other metal oxides such as K [14,16], Zn [17], Mg [18], Zr [18] as promoters, which modify the redox and/or the acid–base properties of the catalyst. Tetrahedral vanadium species are predominant in selective Al_2O_3-supported vanadia catalysts. However, due to the relatively low capacity of alumina to disperse the vanadium on its surface [1,4,19], tetrahedral sites are formed at relatively low V-loading catalysts, leading to low productivities of olefins.

The productivity to ethylene of vanadia supported on siliceous MCM-41 has been reported to be higher than that obtained on conventional SiO_2 because of the large surface area of the support [20]. So, the use of other mesoporous materials as support seems to be interesting.

Mesoporous Al_2O_3 has recently been proposed as support in several formulations of catalysts [21–23]. Since the reactivity of alumina-supported vanadia catalysts is higher than of those supported on silica, an alternative way to achieve higher productivities could be the use of mesoporous Al_2O_3. The aim of this paper is to investigate the nature of the V-species formed by impregnation on a mesoporous

* Corresponding author. Fax: +34 96 3877809.
E-mail address: jmlopez@itq.upv.es (J.M. López Nieto).
[1] On leave from Dipartimento di Chimica Industriale e dei Materiali, Universitá di Bologna, Vle. Risorgimento 4, 40136 Bologna, Italy.

0920-5861/$ – see front matter © 2004 Elsevier B.V. All rights reserved.
doi:10.1016/j.cattod.2004.06.151

Al_2O_3 with an alcoholic solution, and to study the catalytic results in the oxidative dehydrogenation of ethane. We shall show that the productivity to olefins is higher than on γ-Al_2O_3 support as a result of its larger surface area.

2. Experimental

2.1. Catalyst preparation

Mesoporous Al_2O_3 (MAL) has been synthesized in propanolic media using estearic acid as surfactant and aluminium trisecbutoxide (ASB) as the inorganic aluminium source [23]. The surfactant was dissolved in propanol at 313 K under stirring, adding the appropriate amount of water to obtain the final gel composition. Then, ASB was added and the gel was left under stirring during 10 min at 313 K. The gel was prepared with a final ASB/estearic acid/propanol/water molar ratio of 1:0.32:26:3.25.

The crystallization was carried out in an oven at 373 K during 48 h at autogenous pressure of the synthesis gel. The as-made alumina was obtained by filtration, and washed with ethanol to eliminate the non-reacted surfactant. The resulting solid is dried at 333 K, and finally calcined at 623 K (2 h).

Vanadia supported on the mesoporous Al_2O_3 catalysts were prepared by following a wet impregnation method. An ethanolic solution of vanadyl acetylacetonate, with the amount of vanadium necessary in order to achieve a final V-content of 2.4–24.1 wt.% of V-atoms, was contacted with the mesoporous carrier. The ethanol was then rotaevaporated until complete dryness. The dried samples were then calcined at 873 K for 6 h. The samples are named as XV-MAL in which X corresponds to the theoretical V-coverage. The characteristics of calcined catalysts are summarized in Table 1. For comparison, a vanadia supported on alumina (Girdler T126 γ-Al_2O_3 support; S_{BET} = 188 $m^2\,g^{-1}$) was also prepared by percolating a 0.05 M ammonium metavanadate solution through γ-Al_2O_3 support (400 ml of solution for 5 g of the support) at a final pH of 7 [10]. The sample was named as 36V-AL.

2.2. Catalyst characterization

N_2 and Ar adsorption isotherms were determined in an ASAP 2010 instrument at 77 and 87 K, respectively, after degassing the samples (1.33 10^{-2} Pa) at 673 K, overnight.

X-ray diffraction patterns (XRD) were collected on a Philips X'Pert diffractometer equipped with a secondary graphite monochromator, operating at 40 kV and 45 mA and employing nickel-filtered Cu Kα radiation (λ = 0.1542 nm).

Diffuse reflectance-UV–vis spectra were collected on a Cary 5 equipped with a 'Prayting Mantis' attachment from Harric. The sample cell was equipped with a reaction chamber that allows ''in situ'' experiments at high temperature and under controlled atmosphere. The samples were dehydrated ''in situ'' in dry air at 673 K for 30 min. The spectra were recorded upon cooling down to room temperature flowing dry air through the sample to avoid rehydration processes.

Solid state ^{51}V NMR spectra were recorded at room temperature with a Bruker Avance 400 spectrometer. Wide-line spectra under static conditions were acquired with a BL7 Bruker probe, using pulses of 1 μs to flip the magnetization $\pi/20$ rad, and a recycle delay of 2 s. The spectra of the samples spinning at 30 KHz at the magic angle (MAS) were measured using pulses of 0.5 μs corresponding to a flip angle of $\pi/13$ rad, with a recycle delay of 2 s, using a 2.5 mm Bruker probe. The ^{51}V chemical shifts are referred to liquid $VOCl_3$, using $Mg_3V_2O_8$ (δ = −554 ppm) as secondary reference.

Temperature-programmed reduction (TPR) spectra were obtained on a 2910 Micromeritics apparatus loaded with 100 mg of catalyst. The samples were first treated in argon at room temperature during 1 h. The samples were subsequently contacted with an H_2/Ar mixture (H_2/Ar molar ratio of 0.10 and a total flow of 50 ml min^{-1}) and heated, at a rate of 10 K min^{-1}, to a final temperature of 973 K.

Table 1
Characteristics of supported vanadia catalysts

Sample	V-loading[a] (wt.%)	BET surface area ($m^2\,g^{-1}$)	Pore size (Å)	Theoretical surface coverage, θ[b]	H_2-TPR results[c]		
					T_M (K)	H_2-uptake[d]	AOS
MAL	0	572	40	0.0	–	–	–
5V-MAL	2.4	435	nd	5.0	763	3.4	3.5
20V-MAL	9.7	256	37	20	748	12.1	3.7
36V-MAL	17.4	244	37	36	748	21.7	3.7
50V-MAL	24.1	200	33	50	748	27.3	3.9
γ-Al_2O_3	0	188	nd	0.0	–	–	–
36V-AL	4.3	137	nd	36[e]	748	5.1	3.8

[a] Vanadium content, in wt.% of V-atoms, was determined by atomic absorption spectrometry.
[b] θ, theoretical vanadium superficial coverage (calculated for the unit surface area) have been obtained assuming the theoretical monolayer of vanadium to be 4.98 × 10^{18} molecules V_2O_5 cm^{-2} [15].
[c] Temperature of the maximum hydrogen consumption (T_M) and the average oxidation state (AOS) after reduction.
[d] H_2-uptake in mmol g^{-1}.
[e] Taking into account a surface area of the support of 188 $m^2\,g^{-1}$.

Infrared spectra of adsorbed pyridine were obtained in a Nicolet 710 FT-IR spectrophotometer. Wafers of 10 mg/cm^2 were mounted in a pyrex vacuum cell fitted with CaF_2 windows. The samples were pretreated overnight at 673 K and then cooled at room temperature (rt) to obtain the original IR spectra. Then, pyridine was admitted at room temperature, and subsequently degassed at 423 and 523 K for 1 h and the spectra registered at room temperature.

2.3. Catalytic tests

The catalytic experiments were carried out in a fixed bed quartz tubular reactor, working at atmospheric pressure, and equipped with a coaxial thermocouple for catalytic bed temperature profiling. Catalyst samples (0.3–0.5 mm particle size) were introduced in the reactor. The flow rate and the amount of catalyst were varied in order to achieve different propane conversion levels. The feed consisted of a mixture of ethane/oxygen/helium with a molar ratio 4/8/88. Experiments were carried out in the 793–873 K temperature interval. Reactants and reaction products were analyzed by on-line gas chromatography [20].

3. Results and discussion

3.1. Catalyst characterization

Catalysts were prepared by V impregnation on mesoporous Al_2O_3 and subsequent calcination, up to a vanadium content close to 24.1 wt.% of V-atoms, which corresponds to ca. 50% of the theoretical monolayer of vanadia on the surface of the support (Table 1). The XRD patterns of the alumina-supported vanadia samples (V-loadings from 2.4 to 17.4 wt.%) are well-defined and characteristic of the mesoporous phase (Fig. 1), although some crystallinity loss occurs at high V-loading. This conclusion is supported by the relatively high surface areas (S_{BET}) and the very narrow pore size distributions (Table 1), and the high adsorption capacity observed in catalysts (Fig. 2). However, the mesoporous could partially colapse on samples with V-loadings higher than 36% of the theoretical vanadia monolayer, whereas the meso-structure is not preserved at coverages above 50%.

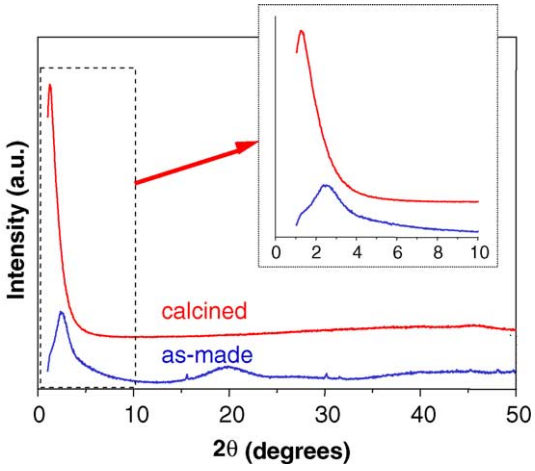

Fig. 1. XRD pattern of vanadia supported on mesoporous Al_2O_3 catalysts (20V-MAL sample).

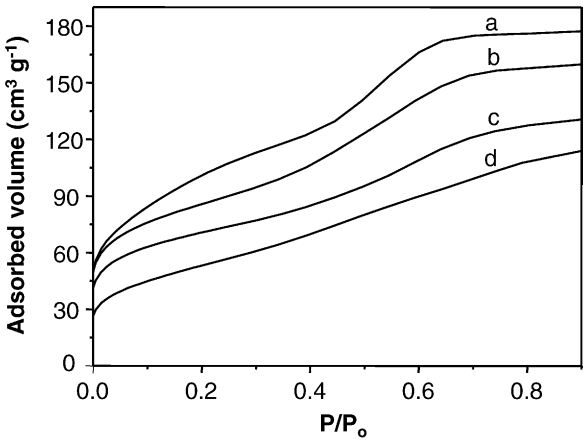

Fig. 2. Adsorption capacity of vanadia supported on mesoporous alumina with V-loading of 0 (a), 20 (b), 36 (c) and 50 (d) of the theoretical vanadia monolayer. The characteristics of catalysts are shown in Table 1.

Fig. 3 shows the DR-UV–vis spectra of the calcined catalysts. The sample with the lower V-content shows a maximum at 277 nm, which shifts to higher wavelengths when the V-loading increases, reaching 322 nm in the sample with 17.4 wt.% of V-atoms (Fig. 3). The absorption band in the region 280–290 nm indicates the presence of isolated tetrahedral V^{5+} species, while in the range 300–330 nm can be related to polymeric tetrahedral V^{5+} species [10,13]. An additional band in the region 400–450 nm is clearly observed for sample 50V-MAL, while it is weak in the sample 36V-MAL, and absent below the 36% of the theoretical superficial coverage. This band can be related to

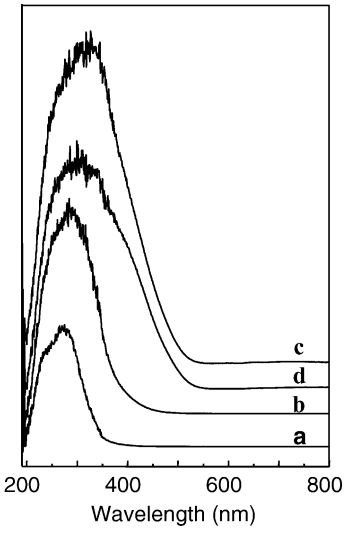

Fig. 3. DR-UV–vis spectra of vanadia supported on mesoporous Al_2O_3 catalysts: 5V-MAL (a); 20V-MAL (b); 36V-MAL (c); 50V-MAL (d).

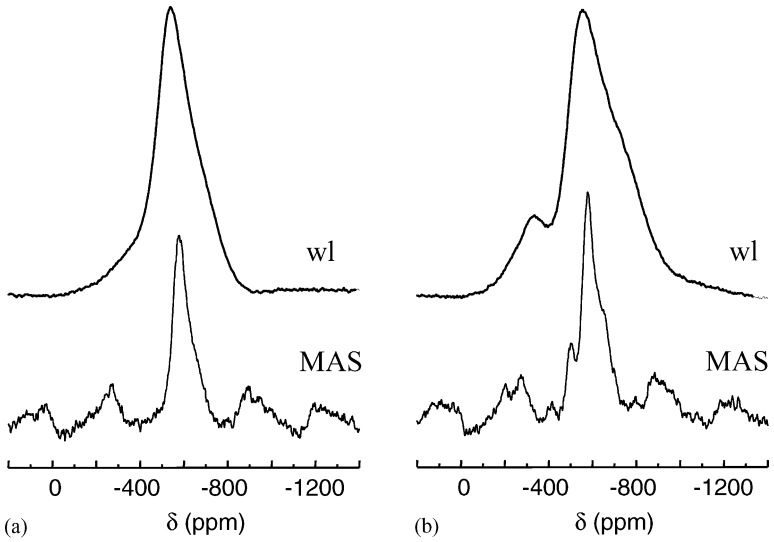

Fig. 4. ^{51}V wide-line (wl) and MAS NMR spectra (spinning rate of 30 kHz) of samples 20V-MAL (a) and 36V-MAL (b).

the presence of "bulk-type" polymeric V_2O_5-like vanadium species [10,13]. So, tetrahedral vanadium V^{5+} species are predominant at V-loading below 17 wt.% of V-atoms (i.e. below 36% of the theoretical monolayer of vanadia on the alumina surface) being isolated only at the lower vanadia coverage. Above this value, octahedral vanadium species predominate.

These results are in good agreement with those previously reported for γ-alumina (Girdler)-supported vanadia catalysts [10], but the different species are formed at higher vanadium contents on mesoporous materials. Thus, it can be concluded that mesoporous alumina behaves similarly to conventional alumina except that permits the incorporation of higher amount of vanadium atoms without the formation of polymeric vanadium species "bulk-type" V_2O_5, because of its higher surface area.

Fig. 4 shows the wide-line and MAS NMR spectra of samples 20V-MAL and 36V-MAL. The static spectrum of sample 20V-MAL consists of a main signal with the maximum at ca. −540 ppm with shoulders at approximately −250 and −700 ppm, which under spinning conditions gives an asymmetric band at −580 ppm. The shape of the static spectrum is very similar to that previously reported by Eckert and Wachs for Al_2O_3-supported vanadia catalysts at low vanadium coverages [24], denoted by the authors as type **b**. The characteristics of this signal allowed its assignment to tetrahedral V^{5+} of $Q^{(2)}$ type, i.e. to polymeric $[O–V(O_2)–]^{2-}$ species [24].

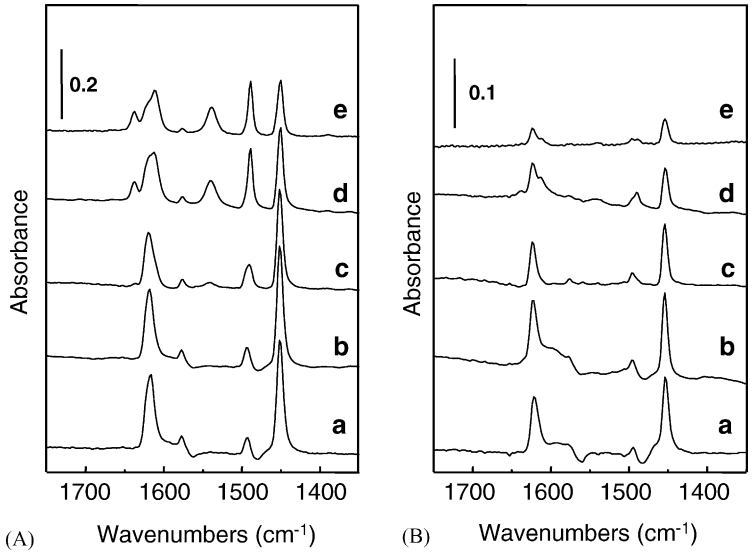

Fig. 5. FT-IR spectra of pyridine adsorbed on vanadia supported on mesoporous Al_2O_3 catalysts after evacuation at 423 K (A) and 523 K (B). Samples: MAL (a); 5V-MAL (b); 20V-MAL (c); 36V-MAL (d); 50V-MAL (e).

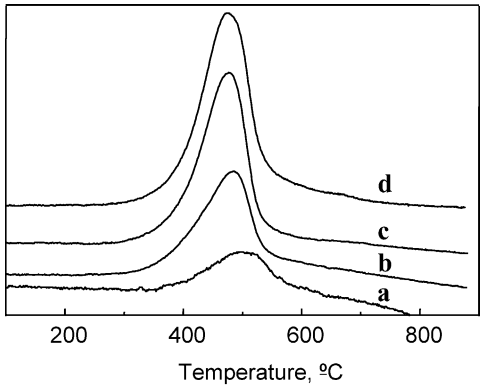

Fig. 6. TPR patterns of vanadia supported on mesoporous Al_2O_3 catalysts. Samples: 5V-MAL (a); 20V-MAL (b); 36V-MAL (c); 50V-MAL (d).

A second signal with the main component at −305 ppm in the wide-line spectrum and a peak at −500 ppm under MAS conditions is observed for sample 36V-MAL, which grows with the vanadium loading. According to Eckert and Wachs [24], this signal denoted by them as **a**, can be attributed to distorted octahedral V^{5+} species. We must note that while signal **a** dominates the spectrum of sample 36V-AL (with a 4.3 wt.% of V-atoms on γ-Al_2O_3 [10]), it is still weak for sample 36V-MAL (with 17.4 wt.% of V-atoms on mesoporous Al_2O_3), clearly indicating that the large surface area of the alumina used here allows to disperse more vanadium on the surface.

The IR spectra of samples possessing low V contents upon degassing pyridine at 423 K (Fig. 5A, spectra a–c) show the presence of bands at 1450, 1492, and 1622 cm^{-1} associated to pyridine coordinated to Lewis acid sites [10,14,25]. Also, a weak band at 1578 cm^{-1} that can be due to some physisorbed pyridine is visible in the spectra. Upon increasing the V-loading, the evolution of characteristic bands of pyridinium cations at 1540 and 1638 cm^{-1} suggest the formation of Brönsted acid sites on V-supported catalysts. The very low acid strength sites is evidenced by the disappearance of these two bands upon desorption at 523 K (Fig. 5B) suggesting that pyridine is retained exclusively on Lewis acid sites. On the other hand, the presence of a new band at 1615 cm^{-1} at high V-loading may indicate the presence of a new type of Lewis acid sites associated to polymeric V-species. It is noticeable that the strength of the Lewis acid sites also decreases as the V-content increases as deduced from the constant diminution of the intensity of the IR band at 523 K.

The TPR patterns of the catalysts supported on mesoporous Al_2O_3 are compared in Fig. 6 and the results collected in Table 1. The maximum of hydrogen consumption appears at ca. 763 K for the sample with the lower V-loading (5V-MAL) and at 748 K for vanadia coverages above 20% of the theoretical monolayer (ca. 10 wt.% of V-atoms) or for vanadia supported on γ-Al_2O_3 (sample 36V-AL).

The average oxidation state (AOS) of vanadium after the TPR experiments, shown in Table 1, is of ca. 3.8 in all the catalysts, including the one in which γ-Al_2O_3 is used as a support (sample 36V-AL). These results suggest that the same type vanadium species with similar reducibility must be formed on alumina for a specific theoretical coverage of vanadia, independently on the surface area of the support.

3.2. Oxidative dehydrogenation of ethane

The catalytic results obtained in the oxidative dehydrogenation of ethane over supported vanadia catalysts are shown in Table 2. Ethylene, CO and CO_2 are the main reaction products. No oxygenated products other than carbon oxides have been observed.

Fig. 7 shows the variation of the ethane conversion and the selectivity to the main reaction products (ethylene, CO and CO_2) with the reaction temperature. The highest ethane conversion is obtained on sample 36V-MAL, while the highest selectivity to ethylene is achieved on sample 20V-MAL. The inspection of Fig. 7 shows that the selectivity to CO increases with the V-loading, whereas the selectivity to CO_2 is similar for all catalysts except for 5V-MAL, which is much higher. Therefore, besides ethylene, carbon dioxide and carbon monoxide are mainly observed on catalysts with low and high vanadium coverages, respectively.

Fig. 8 depicts the variation of the yield of ethylene with the reaction temperature. The catalysts with high V-content (36V-MAL and 50V-MAL) give the highest yield of ethylene at low reaction temperature (and low ethane conversions), whereas sample 20V-MAL is the most active at high temperature (and high ethane conversions). This is also

Table 2
Catalytic performance of supported vanadia catalysts

Sample	W/F[a]	C_2H_6 conversion[b] (%)	Selectivity (%)			C_2H_4 yield (%)	$STY_{C_2H_4}$[c]
			C_2H_4	CO	CO_2		
MAL	10	5	8.0	35.8	56.2	0.4	11.2
20V-MAL	10	24.9	63.4	25.1	11.5	15.8	445
36V-MAL	10	59.4	26.2	54.1	19.6	15.6	437
γ-Al_2O_3	26	8	8.1	38.9	54.8	0.6	6.5
36V-AL	26	42	48.9	43.8	7.4	20.5	224

[a] Contact time, W/F, in $g_{cat}\,h\,mol_{C_2}^{-1}$.
[b] Reaction temperature = 843 K.
[c] Space time yield ($STY_{C_2H_4}$) in $g_{C_2H_4}\,kg_{cat}\,h^{-1}$.

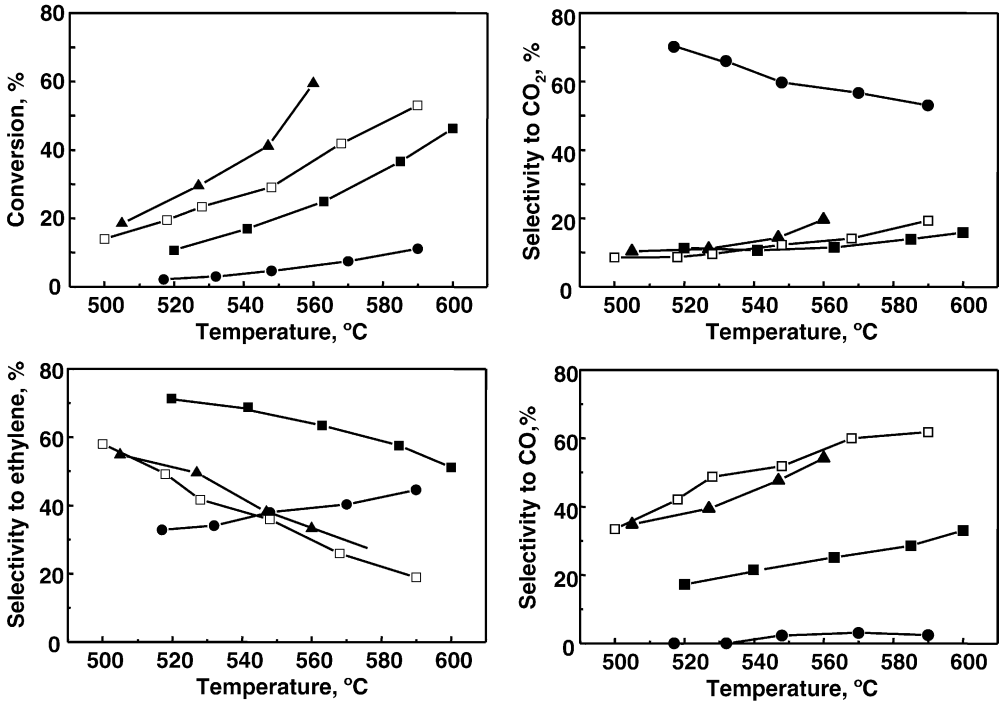

Fig. 7. Catalytic results obtained during the oxidative dehydrogenation of ethane on mesoporous Al_2O_3-supported vanadia catalysts: 5V-MAL (●); 20V-MAL (■); 36V-MAL (▲); 50V-MAL (□). Experimental conditions: ethane/oxygen/helium with a molar ratio 4/8/88; contact time, *W*/*F*, of 10 g_{cat} h $mol_{C_2}^{-1}$.

confirmed from the data obtained at iso-conversion conditions (Fig. 9), in which the highest selectivity to ethylene and the highest yield of ethylene is achieved on sample 20V-MAL. These results suggest that the ethylene combustion on samples with high V-contents is higher than on catalysts with low V-loading.

According to these results, a reaction network with both parallel and consecutive reaction can be proposed, in agreement with previously reported results [10]. CO_2 comes from the oxidation of propane over the support, and then is mainly formed at low V-coverage; CO is formed from ethylene over highly coordinated V-species, more abundant at high V-coverage. The best catalytic results on sample 20V-MAL, with a V-coverage of 20% of the theoretical monolayer, can be explained by the relatively high dispersion of vanadium, which gives lower formation of carbon oxides from the deep oxidation of both ethane and ethylene.

It has been reported that the highest selectivity to ethylene during the ODH of ethane on alumina-supported vanadia catalysts using a commercial γ-Al_2O_3 with low surface area, is also achieved at 20–30% of the theoretical monolayer [10]. According to the results of Table 2, the 20V-MAL

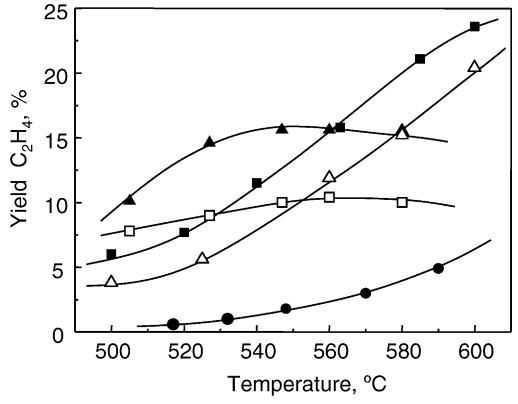

Fig. 8. Variation of the yield of ethylene with the reaction temperature obtained during the oxidative dehydrogenation of ethane on mesoporous Al_2O_3-supported vanadia catalysts: 5V-MAL (●); 20V-MAL (■); 36V-MAL (▲); 50V-MAL (□); 36V-AL (△).

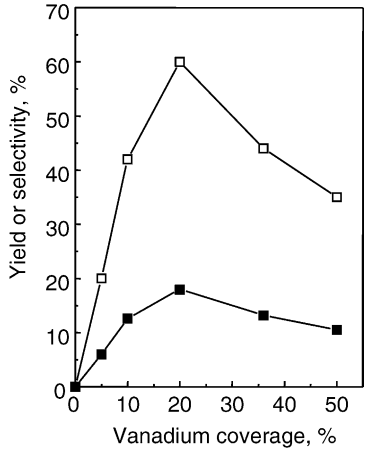

Fig. 9. Variation of the selectivity of ethylene (□) and the yield of ethylene (■) with the V-coverage of mesoporous Al_2O_3-supported vanadia catalysts obtained during the ODH of ethane at 843 K and an ethane conversion of 30%.

sample presents a space time yield ($STY_{C_2H_4}$) of ca. 445 $g_{C_2H_4}$ kg_{cat} h^{-1}, keeping selectivities to ethylene about 63%. However, the space time yield ($STY_{C_2H_4}$) obtained on vanadia supported on γ-Al_2O_3 (36V-AL sample) is ca. 224 $g_{C_2H_4}$ kg_{cat} h^{-1}, keeping selectivities to ethylene about 49%, was obtained 843 K. These catalytic results suggest that the formation of ethylene on vanadia supported on mesoporous Al_2O_3 is higher than on the corresponding VO_x/γ-Al_2O_3 catalysts.

4. Discussion

^{51}V NMR and DR-UV–vis spectroscopic techniques have been applied to characterize the nature of the vanadium species in mesoporous alumina-supported catalysts. The results show that tetrahedral V^{5+} species are predominant at V-coverage below 50%, isolated in the catalyst 5V-MAL and polymeric at higher V-loading (samples 20V-MAL and 36V-MAL). Octahedral V^{5+} involved in an oxidic phase is also observed only at high vanadium contents (higher than the 30% of the theoretical monolayer). The same species are formed when γ-Al_2O_3 are used as a support [10]. The TPR patterns show that the reducibility of vanadia supported on mesoporous alumina is similar to that on γ-Al_2O_3, again pointing out that the same types of vanadium species are present on both supports.

These results suggest that vanadium species are dispersed during the impregnation step in the same manner than on γ-Al_2O_3-supported catalysts. Since similar physico-chemical properties have been observed in both series, one could expect similar catalytic behavior. Both the selectivity to ethylene and the space time yields for the ODH of ethane to ethylene on vanadia supported on mesoporous alumina is higher than on γ-Al_2O_3 because of the dispersion of vanadium on the support. However, the specific activity per V-atom is lower on mesoporous alumina-supported catalysts. This could be explained by considering that a partial collapse of the mesoporous structured during the calcination step decreases the number of accessible V-atoms, but this occurs without formation of the non-selective V_2O_5 (no V_2O_5 was observed in our catalysts). In all cases, the mesoporous alumina-supported vanadia catalysts are more effective in the ODH of ethane to ethylene as a consequence of the higher selectivity to ethylene on these catalysts.

In agreement with the catalytic results obtained during the oxidation of ethane, the following reaction network can be proposed:

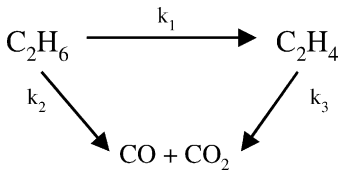

Ethylene is the most abundant primary product while CO and CO_2 comes from the deep oxidation of both ethane and ethylene. This reaction pathway is similar to those previously reported for supported vanadia catalyst [1,10,26]. The higher yield at low temperatures (and low ethane conversions) are achieved on samples 36V-MAL and 50V-MAL, while the higher yield at high temperatures (i.e. high ethane conversion) are achieved on samples 20V-MAL and 5V-MAL (Fig. 8). This can be explained by considering the nature of the vanadium species in each catalysts. Octahedral V^{5+} species, active in ethane oxidation but also in ethylene combustion, are mainly present in both 36V-MAL and 50V-MAL. However, tetrahedral V^{5+} species, present mainly in 20V-MAL and 5V-MAL samples, presenting k_1/k_3 and k_1/k_2 ratios higher than on vanadia supported on γ-Al_2O_3 (36V-AL sample), are less active but more selective.

So, the high selectivities to oxydehydrogenation product on sample 20V-MAL is a consequence of the high dispersion of vanadium. Polymeric tetrahedral V^{5+} species appears to be the selective sites in the oxidative dehydrogenation of ethane, as it has previously been proposed in VO_x/γ-Al_2O_3 [10–15]. At higher V-loading, octahedral vanadium species and Brönsted acid sites appear, which have a negative effect on the selectivity to ethylene, favoring a higher deep oxidation of ethylene and the formation of carbon monoxide.

In conclusion, vanadia catalysts supported on mesoporous alumina are active and selective in the oxidative dehydrogenation of ethane. The V^{5+} species are similar than those reported in VO_x/γ-Al_2O_3 catalysts, when compared at the same V-coverage. The catalytic results are related to the amount of V-atoms dispersed (and with a tetrahedral coordination) on the surface of the support, which depend on both the high surface area and the number of hydroxyl groups of the oxide support. In this way, high productivities to ethylene can be achieved during the oxidative dehydrogenation of ethane keeping selectivities to ethylene higher than on vanadia supported on γ-Al_2O_3 (36V-AL sample).

Acknowledgment

Financial support from DGICYT, Spain (Projects PPQ2003-03946 and MAT 2003-07769-CO2-01) is gratefully acknowledged.

References

[1] T. Blasco, J.M. López Nieto, Appl. Catal. A: Gen. 157 (1997) 117.
[2] F. Cavani, F. Trifiró, Catal. Today 24 (1995) 307.
[3] M. Bañares, Catal. Today 51 (1999) 319.
[4] X. Gao, I.E. Wachs, Top. Catal. 18 (2002) 243.
[5] V.V. Guliants, Catal. Today 51 (1999) 255.
[6] I.E. Wachs, B.M. Weckhuysen, Appl. Catal. A: Gen. 157 (1997) 67.
[7] G. Centi, S. Perhatoner, F. Trifiró, Res. Chem. Intermed. 5 (1991) 49.
[8] P. Concepción, A. Galli, J.M. López Nieto, A. Dejoz, M.I. Vázquez, Top. Catal. 3 (1996) 451.

[9] T. Blasco, J.M. López Nieto, A. Dejoz, M.I. Vázquez, J. Catal. 157 (1995) 271.
[10] T. Blasco, A. Galli, J.M. López Nieto, F. Trifiró, J. Catal. 169 (1997) 203.
[11] J. Le Bars, A. Auroux, M. Forissier, J.C. Vedrine, J. Catal. 162 (1996) 250.
[12] X. Gao, M.A. Bañares, I.E. Wachs, J. Catal. 188 (1999) 325.
[13] J.G. Eon, R. Olier, J.C. Volta, J. Catal. 145 (1994) 318.
[14] R. Coenraads, J.M. López Nieto, A. Dejoz, M.I. Vázquez, Stud. Surf. Sci. Catal. 110 (1997) 443.
[15] G. Capanelli, E. Carosini, F. Cavani, O. Monticelli, F. Trifiró, Chem. Eng. Sci. 51 (1996) 1817.
[16] A. Galli, J.M. López Nieto, A. Dejoz, M.I. Vazquez, Catal. Lett. 34 (1995) 51.
[17] A.R.L.M. Mattos, R.A.S.S. Gil, M.L.M. Rocco, J.G. Eon, J. Mol. Catal. A: Chem. 178 (2002) 229.
[18] M.E. Harlin, V.M. Niemi, A.O.I. Ktase, B.M. Weckhuysen, J. Catal. 203 (2001) 242.
[19] J.M. López Nieto, G. Kremenic, J.L.G. Fierro, Appl. Catal. 61 (1990) 235.
[20] B. Solsona, T. Blasco, J.M. López Nieto, M.L. Peña, F. Rey, A. Vidal-Moya, J. Catal. 203 (2001) 443.
[21] J. Cejka, P.J. Kooyman, L. Vesela, J. Rathowsky, A. Zukal, Phys. Chem. Chem. Phys. 4 (2002) 4823.
[22] V. Gonzalez-Peña, C. Márquez-Alvarez, E. Sastre, J. Pérez-Pariente, Stud. Surf. Sci. Catal. 135 (2001) 1072.
[23] F. Vaudry, S. Khodabandeh, M.E. Davis, Chem. Mater. 8 (1996) 1451.
[24] H. Eckert, I.E. Wachs, J. Phys. Chem. 93 (1989) 6796.
[25] J. Le Bars, J.C. Vedrine, A. Auroux, S. Trautmant, M. Baerns, Appl. Catal. A: Gen. 119 (1994) 341.
[26] K. Chen, E. Iglesia, A.T. Bell, J. Catal. 192 (2000) 197.